



VIBRATION SUPPRESSION OF FLEXIBLE SPACECRAFT DURING ATTITUDE CONTROL

GANGBING SONG[†]

Department of Mechanical Engineering, The University of Akron, Akron, OH 44325-3903, USA
and

BRIJ N. AGRAWAL

Aeronautics and Astronautics Department, US Naval Postgraduate School, Monterey, CA 93943, USA

(Received 17 September 1999; revised version received 7 June 2000)

Abstract—This paper presents a new approach to vibration reduction of flexible spacecraft during attitude control by using pulse width pulse frequency (PWPF) modulator for thruster firing and smart materials for active vibration suppression. The experiment was conducted on the Naval Postgraduate School (NPS)'s flexible spacecraft simulator (FSS), which consists of a central rigid body and an L-shape flexible appendage. A pair of on–off thrusters are used to re-orient the FSS. To actively suppress vibrations introduced to the flexible appendage, embedded piezoelectric ceramic patches are used as both sensors and actuators to detect and counter react to the induced vibration. For active vibration suppression using the piezoelectric ceramic patches, positive position feedback (PPF) control targeting at the first two flexible modes of the FSS system is used. Experimental results demonstrate the effectiveness of the control strategy of PWPF modulation for attitude control and PPF for active vibration suppression. © 2001 Elsevier Science Ltd. All rights reserved

1. INTRODUCTION

Modern spacecraft often employ large flexible structures such as solar arrays, while requirement for attitude control performance becomes more stringent. For attitude operations that require small control actions, reaction/momentum wheels are used. However, during orbital correction maneuvers, such as north–south station keeping and slew, the required torque are normally too high for reaction/momentum wheels. Therefore, thrusters are normally used for attitude control during these maneuvers.

Reaction/momentum wheels can provide continuous control action according to the desired torque profile for attitude control. Thrusters, on the other hand are on–off devices and are normally capable of providing only fixed torque. Therefore, achieving high attitude control performance using thrusters is a challenging task. The task becomes even more complicated for flexible spacecraft where thruster firings could excite modes resulting in attitude control instability or limit cycles.

The two major approaches for thruster control are bangbang control and pulse modulation. Bangbang control is simple in formulation, but results in excessive thruster action. Its discontinuous control actions may interact with the flexible modes of spacecraft and result in limit cycles. On the other hand, pulse modulators are commonly employed due to their advantages of reduced propellant consumption and near-linear duty cycle. In general, pulse modulators produce a pulse command sequence to the thruster valves by adjusting pulse width and/or pulse frequency. Pulse modulators such as pseudo-rate modulator [1], integral-pulse frequency modulator [2,3], and pulse-width and pulse-frequency (PWPF) modulator [4–7] have been proposed. Among these, the PWPF modulator holds several superior advantages such as close to linear operation, high accuracy and adjustable pulse width and pulse frequency that provide scope for advanced control.

On–off thruster firing, no matter the method of modulation, will introduce vibrations to the flexible structures to some degree. Effectively suppressing the induced vibration poses a challenging task for spacecraft designers. One promising method for this problem is to use embedded piezoelectric

[†]Corresponding author. Tel.: +1-330-972-6715.
E-mail address: gsong@uakron.edu (G. Song).

materials as actuator (compensator) since piezoelectric materials have the advantages of high stiffness, light weight, low power consumption and easy implementation. A wide range of approaches have been proposed for using piezoelectric material to actively control vibration of flexible structures. Positive position feedback (PPF) [8–11] was applied by feeding the structural position coordinate directly to the compensator and the product of the compensator and a scalar gain positively back to the structure. PPF offers quick damping for a particular mode. PPF is also easy to implement. Analytical and experimental study also demonstrate that PPF possesses robustness to variations in modal frequency [12].

The goals of this research are to propose a new approach to vibration reduction of flexible spacecraft, by using PWPF modulation for attitude control and smart structures for active vibration suppression, and to experimentally study the effect of this new approach on vibration reduction of spacecraft during attitude maneuvers. The experimental object of this research is Naval Postgraduate School's flexible spacecraft simulator (FSS), which is comprised of a rigid central body with on-off type thrusters and a "L"-shape flexible appendage with smart sensors and a smart actuator. The simulator can be fully floated using compressed air and can simulate the motion of a spacecraft about its pitch axis. This paper presents the results of vibration reduction during attitude control of the FSS using PWPF modulation for thruster control and smart structures for active vibration suppression. In this research, a PWPF modulation is used to control the on-off thrusters for attitude maneuver to reduce vibrations introduced to the flexible appendage. This can be considered as a passive means for vibration reduction. Meanwhile, a smart sensor and a smart actuator with PPF control are used to actively suppress vibrations introduced to the flexible appendage by thruster firings. The rest of the paper is organized as follows: Section 2 discusses the FSS setup, including the thrusters, smart structures, vision server system, and the digital data acquisition and real-time control system. Section 3 presents basics about the PWPF modulator. Section 4 introduces the smart structures used in this research and positive position feedback (PPF) control. Section 5 describes the overall control system, which includes two sub-systems: the attitude control sub-system and the active vibration suppression sub-system. Section 6 presents and analyzes the experimental results. Section 7 concludes the paper.

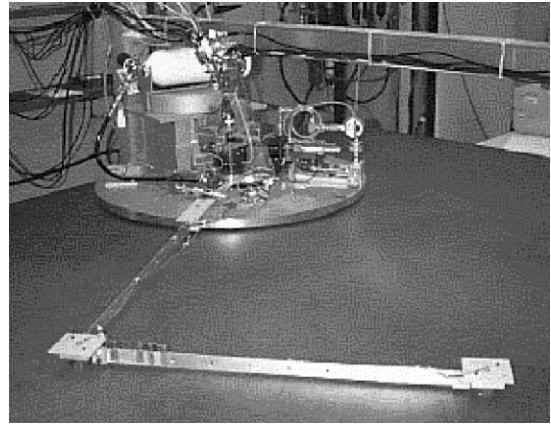


Fig. 1. The flexible spacecraft simulator (FSS) at US Naval Postgraduate School.

2. THE FLEXIBLE SPACECRAFT SIMULATOR

The FSS simulates motion about the pitch axis of a spacecraft. As shown in Fig. 1, it is comprised of a rigid central body and a "L"-shape flexible appendage. The center body represents the main body of the spacecraft while the flexible appendage represents a flexible antenna support structure. The flexible appendage is composed of a base beam cantilevered to the main body and a tip (remote) beam connected to the base beam at a right angle with a rigid elbow joint. The rigid body is supported by three air pads and the flexible appendage is supported by one air pad each at the elbow and tip. These air pads are used to minimize friction. A finite element model experiments reveal that the first two modes are dominant modes for this flexible structure and they are major concerns for vibration reduction. The 1st mode is at 0.30 Hz and the 2nd mode is at 0.93 Hz.

Measurement of the structure states is accomplished by a full complement of sensors. A rotational variable differential transformer (RVDT) mounted on the center axis of the main body measures angular position. Figure 2 shows piezoceramic patches mounted at the root of the base beam and tip beam to measure strain in the flexible appendage. An optical infrared sensing system, as shown in Fig. 3, provides position and rate information for designated LED targets mounted on the structure. Groups of targets are mounted on the main body in addition to the elbow joint and tip of the flexible appendage. This camera is mounted 1.9 m above the granite table assembly. The camera is connected to a 68030 microprocessor running a real-time operating system, *V × Works*. The 12 bit digital data obtained by the camera is ported out of the 68030 via a digital-to-analog (A/D) converter

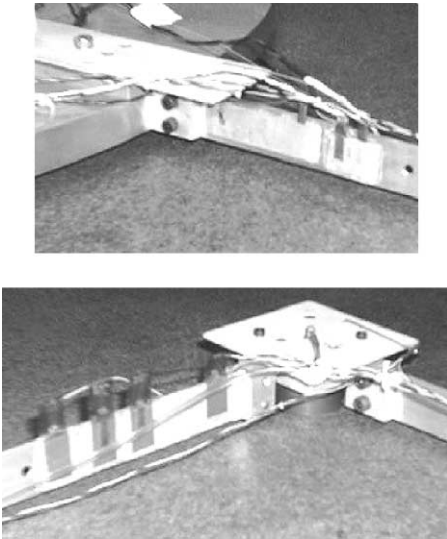


Fig. 2. Base joint (upper) and elbow joint (lower) with piezoceramic actuator and sensor patches and LED targets.

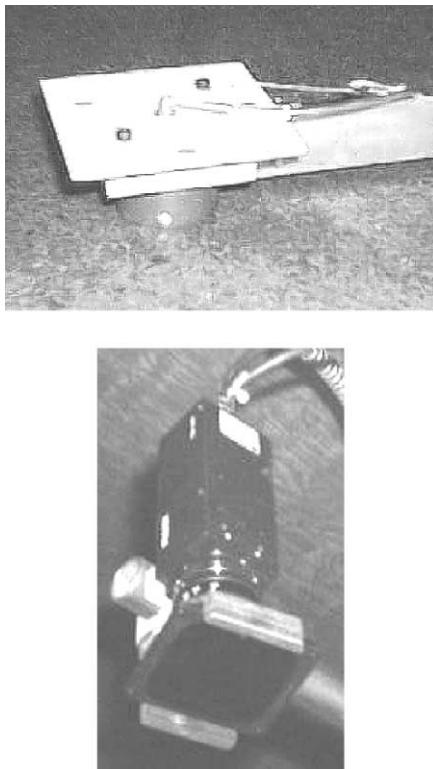


Fig. 3. Flexible appendage tip with LED targets (upper) and optical infrared sensing camera (lower).

card at 60 Hz sampling frequency. The camera's resolution is nominally at the sub-pixel level on the order of 1/20th of a pixel that leads to a camera accuracy of approximately 0.5 mm.

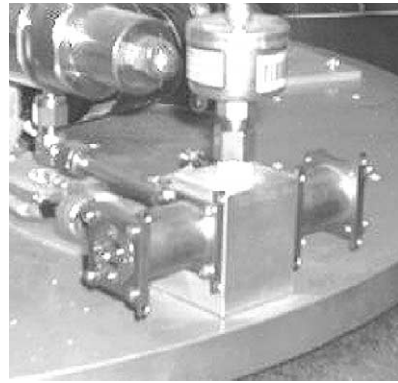


Fig. 4. Cold gas jet thrusters mounted on main body.

Two flight qualified cold gas jet thrusters shown in Fig. 4 are mounted on the main body of the structure to provide high control authority. The two thrusters are on-off types. Located alongside the piezoceramic sensor patches are actuator patches used to provide active damping to the flexible appendage.

Data acquisition and control of the FSS is accomplished with a rapid design prototyping and real time control system; a dSPACE system. The dSPACE system consists of a PC host machine and a TI-C30 real time control processor. Real time code is developed on the host machine via Matlab/Simulink Real time Workshop and is downloaded to the control processor for implementation. Analog sensor signals are accessed by the control processor through an A/D converter. The micro-processor computes the control action according to the downloaded control law and outputs the control action in digital format. The control signal is converted to a analog signals via a digital-to-analog (D/A) converter and sent to the FSS system for implementation. All A/D and D/A inputs are bipolar with a voltage range of ± 10 V. A high voltage power amplifier with a gain of 15 is used to amplify the signal sent to the piezoceramic actuator. This gain on the signal significantly enhances the structural control capabilities without running the risk of de-poling the piezoceramic actuators.

3. PWPF MODULATION

3.1. Basic about PWPF modulator

The PWPF modulator produces a pulse command sequence to the thruster valves by adjusting the pulse width and pulse frequency. In its linear range, the average torque produced equals the demand torque input. Compared with other methods of modulation, PWPF modulator has several

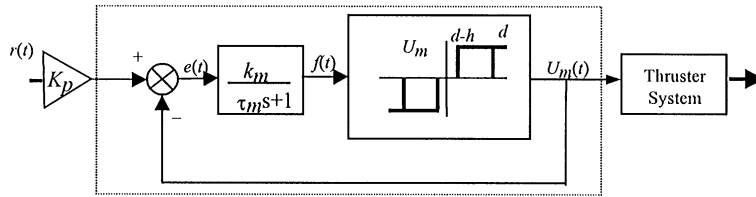


Fig. 5. The PWPF modulator.

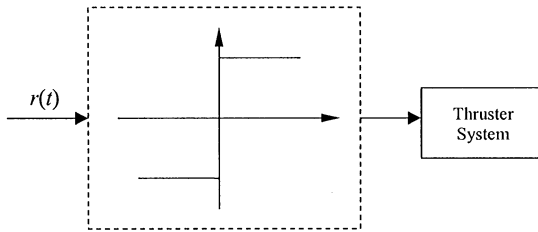


Fig. 6. Bangbang control.

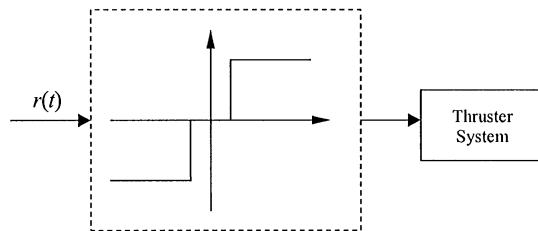


Fig. 7. Bangbang control with deadzone.

superior advantages such as close to linear operation, high accuracy and adjustable PWPF that provide scope for advanced control.

As shown in Fig. 5, the PWPF modulator is comprised of a Schmidt trigger, a pre-filter, and a feedback loop. A Schmidt Trigger is simply an on-off relay with a deadzone and hysteresis. When a positive input to the Schmidt Trigger is greater than d (also denoted as E_{on}), the trigger output is U_m . Consequently, when the input falls below $d-h$ (also denoted as E_{off}), the trigger output is 0. This response is also reflected for negative inputs. The Schmidt Trigger output, U_m , from the feedback loop, and the system input, $r(t)$, form the error signal $e(t)$. The error is fed into the pre-filter whose output $f(t)$ feeds the Schmidt Trigger. The parameters of interest are the pre-filter coefficients k_m and τ_m , input gain K_p , and the Schmidt Trigger parameters d , h , and U_m .

On the other hand, bangbang controller (Fig. 6) can also be used to convert a continuous signal to an on-off type signal that is suitable for thruster control. A variation of a bangbang controller is to use a deadzone (Fig. 7) so that the number of thruster

firings and fuel consumption can be reduced at a possible cost of control accuracy. In this research, the effect of PWPF modulation will be compared with that of bangbang control and deadzoned bangbang control, respectively.

3.2. Selection of PWPF modulator parameters

Selection of PWPF modulator parameters is an important issue. Improper settings of the parameters values will result in large output phase lag, excessive number of thruster firings and fuel consumption and even instability of the system. The design parameters to be studied are the pre-filter coefficients k_m and τ_m , input gain K_p , and the Schmidt Trigger parameters d , h , and U_m . Due to nonlinear nature of the modulator, analytic methods such as describing function cannot produce accurately prediction over a large operation range. Instead, extensive numerical simulations have been carried out to study the effects of these parameters on the performances of the modulator and the FSS [7,13] prior to this research. This paper only presents results from the numerical studies and details on PWPF parameter selection can be found in [13]. Three types of analyses: static analysis, dynamic analysis, and slew analysis are conducted to study different performance indices of the modulator and the rigid-flexible system. The important performance indices of the modulator include modulation factor, thruster cycles (number of thruster firings), a total thruster on-time (fuel consumption). The important performance indices of the FSS include steady state error of the rigid body (indication of the stability), settling time of the rigid body, and modal response of the flexible appendage.

First *static analysis* using constant inputs to the modulator is conducted to study the impact of parameters ($E_{on}(d)$, $E_{off}(d-h)$, k_m and K_p) on the PWPF static performance indices: modulation factor, thruster firing frequency, thruster cycles, and total thruster on-time. To maintain pseudo-linear operation of the PWPF modulator and compromise this objective with total thruster on-time and number of thruster firings, we recommend the

Table 1. Recommended range of PWWF parameters

	Static analysis	Dynamic analysis	Slew analysis	Recommended settings
k_m	$1.0 < 6.0$	N/A	N/A	$1.0 < 6.0$
K_p	$1.0 < 10$	N/A	< 2.0	$1.0 < 2.0$
τ_m	N/A	> 0.1	$0.2 < 0.6$	$0.4 < 0.6$
$E_{on}(d)$	> 0.3	N/A	N/A	> 0.3
$E_{off}(d-h)$	$< 0.8d$	N/A	N/A	$< 0.8d$

preferred range of parameters as listed in Table 1. Then *dynamic analysis* using sinusoidal inputs is conducted to study the effect of the time constant on PWWF output phase lag and thruster activity. It is found that the modulator time constant τ_m should be greater than 2 to avoid excessive thruster firings and fuel consumption. This result is also listed in Table 1. Last, following the recommended parameter settings from both static and dynamic analyses, *slew analysis* is conducted to study the effect of the PWWF parameters on the responses of FSS rigid body and flexible appendage. During the slew analysis, the FSS is required to perform a 10° slew operation with PWWF modulation. Simulations with input gains (K_p) from 1 to 30 and modulator time constants (τ_m) from 0.02 to 0.9 are performed to study the impact of these two parameters on FSS slew performance. Simulations find that these two parameters have a very minimum impact on the steady state error of the rigid body. However, these two parameters dramatically affect rigid body settling time, responses of modes 1 and 2, and number of thruster firings. To keep rigid body settling time small, numerical simulations suggest $\tau_m < 0.6$. To avoid excessive thruster firing, K_p should be less than 5 and τ_m should be greater than 0.1 (consistent with result from dynamic analysis). To minimize responses of flexible modes 1 and 2, simulations suggest that $K_p < 2.0$ and $0.4 < \tau_m < 0.6$. Details of simulations and analysis can be found in [13]. The results from slew analysis are shown in Table 1. Based on the results from static analysis, dynamic analysis, and slew analysis, Table 1 summarizes the recommended ranges for these parameters. The settings in Table 1 can ensure the system's stability while avoiding excessive number of thruster firings and fuel consumption.

4. SMART STRUCTURES AND PPF CONTROL

A smart structure employs distributed actuators and sensors, and one or more microprocessors that analyze the responses from the sensors and use distributed-parameter control theory to command the actuators to apply localized strains to insure the system respond in a desired fashion. A smart

structure has the capability to respond to a changing external environment (such as loads or shape change) as well as to a changing internal environment (such as damage or failure). Smart actuators are used to alter system characteristics (such as stiffness or damping) as well as of system response (such as strain or shape) in a controlled manner. Much of the early development of smart structure technology was driven by space applications such as vibration and shape control of large flexible space structures. Now smart structure research has been extended to aeronautical and other systems.

Piezoceramic material will be used in this research as a sensor to detect and as an actuator to suppress structural vibration. Piezoceramic material possesses the property of piezoelectricity, which describes the phenomenon of generating an electric charge in a material when subjected to a mechanical stress (direct effect), and conversely, generating a mechanical strain in response to an applied electric field. This property prepares piezoceramic materials to function as both sensors and actuators. The advantages of piezoceramic include high efficiency, no moving parts, fast response, and compact size. A commonly used piezoceramic is the lead zirconate titanate (PZT), which has a strong piezo-effect. PZT can be fabricated into different shapes to meet specific geometric requirements. PZT patches are often used as both sensors and actuators, which can be integrated into structures. PZT actuation strain can be on the order of $1000 \mu\text{strain}$. Within the linear range PZT actuators produce strains that are proportional to the applied electric field/voltage. These features make them attractive for structural control applications. The FSS is equipped with two PZT patches as sensors bonded on the roots of both the base beam and the remote beam. One PZT patch is also bonded to the root of the base beam to function as an actuator.

For active vibration control of the flexible appendage, the PPF control scheme shown in Fig. 8 is well suited to implementation utilizing the piezoelectric sensors and actuators. In PPF control methods, structural position information is fed to a compensator. The output of the compensator, magnified by a gain, is fed directly back to the structure. The

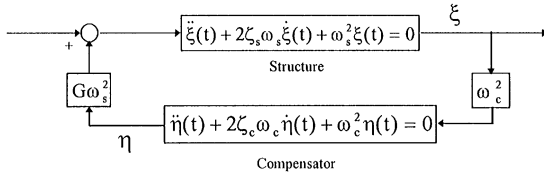


Fig. 8. Positive position feedback block diagram.

equations describing PPF operation are give as

$$\begin{aligned} \ddot{\xi}(t) + 2\zeta_s\omega_s\dot{\xi}(t) + \omega_s^2\xi(t) &= G\omega_s^2\eta, \\ \ddot{\eta}(t) + 2\zeta_c\omega_c\dot{\eta}(t) + \omega_c^2\eta(t) &= \omega_c^2\xi, \end{aligned} \quad (1)$$

where ξ is a coordinate describing displacement of the structure, ζ_s is the damping ratio of the structure, ω_s is the natural frequency of the structure, G is a feedback gain, η is the compensator coordinate, ζ_c is the compensator damping ratio, and ω_c is the frequency of the compensator.

The stability condition for the combined system in eqn (1) is given as

$$\frac{\zeta_s\omega_s^3 + \zeta_c\omega_c^3 + 4\zeta_s\omega_s\zeta_c\omega_c^2}{(\zeta_s\omega_s + \zeta_c\omega_c)^2\omega_s\omega_c} < G < 1.$$

For more interpretation of the PPF compensator, we introduce a frequency domain analysis. Assume ξ is given as

$$\xi(t) = X e^{i\omega_s t},$$

then the output of the compensator is

$$\eta(t) = \frac{X\omega_s/\omega_c e^{i(\omega_s t - \phi)}}{\sqrt{(1 - \omega_s^2/\omega_c^2)^2 + (2\zeta_c\omega_s/\omega_c)^2}},$$

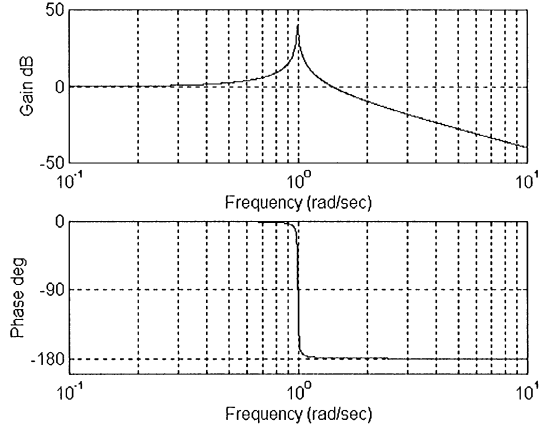
where the phase angle ϕ is

$$\phi = \tan^{-1} \left(\frac{2\zeta_c\omega_s/\omega_c}{1 - \omega_s^2/\omega_c^2} \right).$$

Therefore,

$$\frac{\eta}{\xi} = \frac{e^{-i\phi}}{\sqrt{(1 - \omega_s^2/\omega_c^2)^2 + (2\zeta_c\omega_s/\omega_c)^2}}. \quad (2)$$

The system frequency response characteristics are shown in Fig. 9. It is seen in the figure, when the PPF compensator's frequency is in the region of the structure's natural frequency, the structure experiences active damping. Additionally, when ω_c is lower than ω_s , active flexibility results and when ω_c is larger than ω_s , active stiffness results. Clearly, to maximize damping in the structure, the compensator's frequency should be closely matched to ω_s . Analytical and experimental study of active vibration control of a flexible beam using PPF compensator reveal that PPF compensator with a relative high damping ration is robust to variations in modal frequencies [12]. This is another reason why PPF is adopted in this research.

Fig. 9. Frequency response of system to PPF controller $\omega_s = 1$ rad/s, $\zeta_s = 0.005$, $G = 1$.

5. VIBRATION REDUCTION FOR FSS ATTITUDE CONTROL USING PVPF MODULATOR AND PPF CONTROL

The control system for vibration reduction of the FSS during attitude maneuvers consists of two sub-systems, the attitude control sub-system using PVPF modulation and the active vibration suppression sub-system using smart structures, as shown in Fig. 10. The attitude feedback control sub-system employs a proportional plus derivative (PD) controller and the active vibration suppression sub-system uses positive position feedback control strategy. The attitude control sub-system provides a means for passive vibration control by using PVPF modulation to reduce vibrations introduced to FSS due to thruster firing. The active vibration suppression uses the PZT sensor and actuator to actively cancel the thruster-firing-induced vibration on the flexible appendage. These two sub-systems work together to reduce vibrations during attitude maneuver operations, such as slew and station keeping.

In the attitude control sub-system, the RVDT sensor detects the angular displacement of the FSS rigid body and then, via an A/D converter, the signal is sent to the dSPACE system, where the signal is digitally processed by a low-pass filter and a differentiator. The processed signal is then used to produce a proportional plus derivative (PD) control action. Before being sent to the D/A converter, the PD control signal is converted to on-off signals by a digital PVPF modulator. Finally, the on-off signals are sent to the thrusters to implement the control action and to reorient the FSS.

In the active vibration suppression sub-system, the PZT sensor bonded at the root of the base beam of flexible appendage detects the vibration of the appendage and the signal is then sent to the DSP

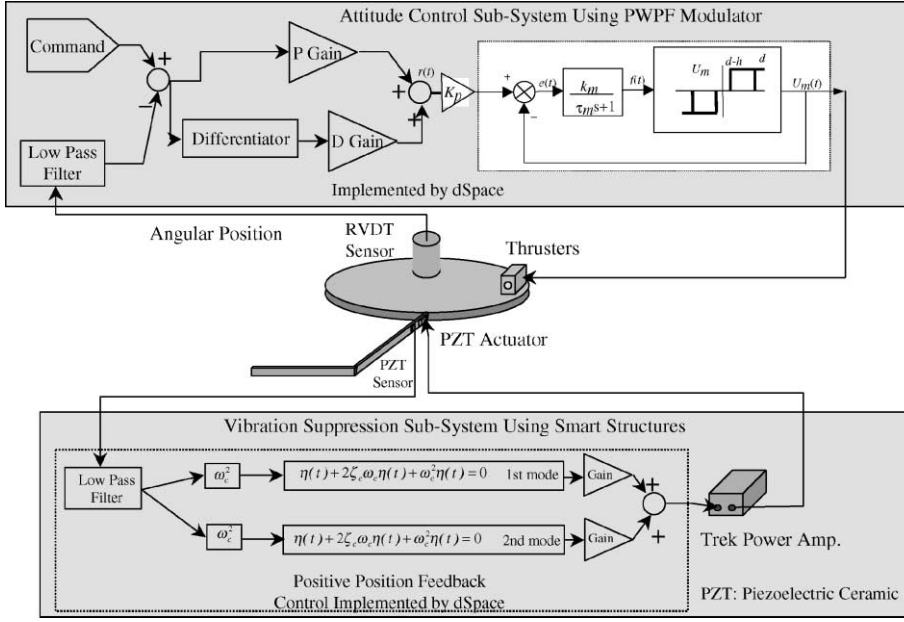


Fig. 10. The block diagram illustrating the control system for FSS vibration reduction.

via an A/D converter. After a low-pass filter, the signal is used by two positive position controllers, targeting at the first two modes of the FSS system modes, to produce control signal. After the D/A converter, the control signal is amplified via a trek voltage amplifier and then fed to the PZT actuator to actively suppress vibrations of the flexible appendage.

During the experiment, the vision server system is used to record the global position of the tip, elbow, and base of the flexible appendage.

6. EXPERIMENTAL RESULTS

6.1. Slew maneuver

In this experiment, the FSS is commanded to perform a 30° slew. For comparative purposes, four different cases of a 30° slew of the FSS are conducted: (1) slew using PWWF modulation and active vibration suppression, (2) slew using bang-bang control (no deadzone) and active vibration suppression, (3) slew using deadzoned-bangbang control and active vibration suppression, and (4) slew using PWWF modulation but without active vibration suppression. Case (1) is compared against cases (2) and (3) to demonstrate the advantages of PWWF modulation for attitude control over bang-bang control with or without deadzone. On the other hand, case (1) is compared with case (4) to show the effectiveness of active vibration suppression of thruster-firing-induced vibration using

Table 2. PPF modulator parameters

Parameter	Value
K_m	1.25
K_p	1.0
τ_m	0.5
$E_{on}(d)$	0.45
$E_{off}(d-h)$	0.20

Table 3. PPF controller parameters

Parameter	1st mode	2nd mode
Targetted frequency (ω_c)	0.3 Hz	0.9 Hz
Gain ($G\omega_c^2$)	5	5
Damping ration (ζ_c)	0.75	0.20

smart structures during attitude control. The proportional gain and the derivative gain of the PD controller for attitude control are 10 and 100, respectively. The PWWF modulator parameters are given in Table 2 based on recommendations from Table 1 and experimental trials. In addition, U_m is set to 2.0. PPF controller parameters are given in Table 3. It can be easily verified that the stability condition for the PPF controller is satisfied for both modes 1 and 2.

First, the PWWF modulator is employed in the attitude control subsystem to slew the FSS for 30° with active vibration suppression using PZT actuator and sensors. The angular displacement of the rigid body along with vibrations of both base beam and remote beam are shown in Fig. 11. The angular displacement signal of the rigid body is obtained

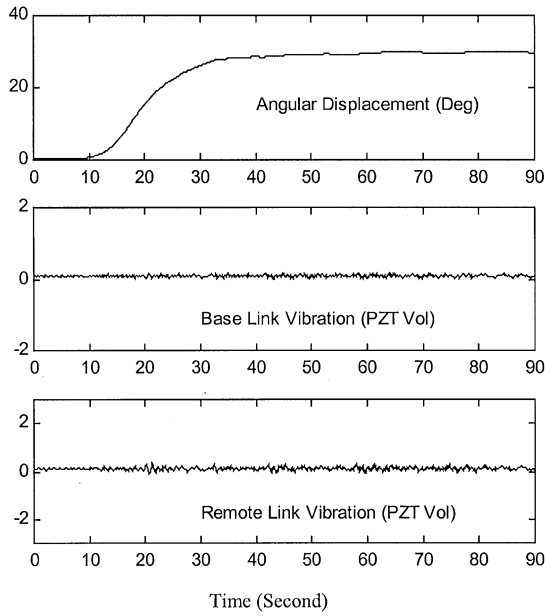


Fig. 11. Slew with PWPf modulation and active vibration suppression.

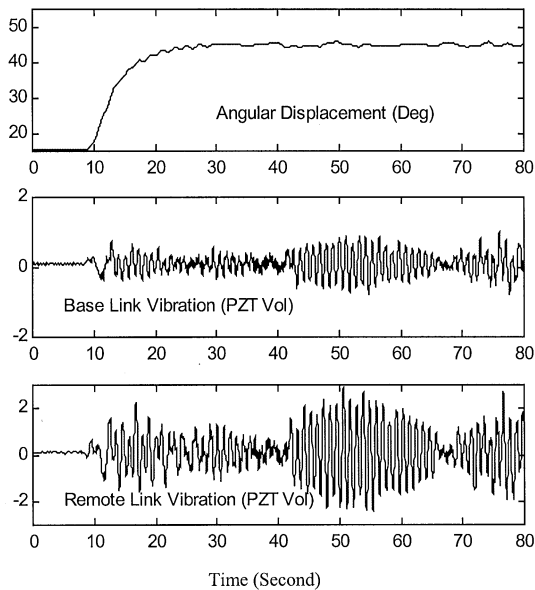


Fig. 12. Slew with bangbang control (no deadzone) and active vibration suppression.

from the RVDT sensor. The vibration signals for both the base beam and the remote beam are obtained from the PZT patch sensors bonded to the root of the two beams. Then, the same experiment is repeated with a bangbang controller replacing the PWPf modulator and the experimental results are shown in Fig. 12. It is clear that, from comparison of Figs. 11 and 12, the thruster firing under PWPf

modulator introduces much less vibration to both the rigid body and the flexible appendage than the bangbang control does. Also excessive thruster firing is observed for the bangbang control. A comparison of the power spectrum density (PSD) plots for these two cases is shown in Fig. 13. The remote sensor data are used for the PSD plots. With the PWPf modulation, the energy levels for the first three modes are about 18, 30, and 15 dB less than those with bangbang control. Using the overhead vision server camera, the tip, elbow and base positions of the flexible appendage are recorded. Figures 14 and 15 show these results for two 30° slew with PWPf modulation and bangbang control, respectively. The trace of the tip position in Fig. 14 is smoother and less oscillatory as compared with that in Fig. 15. This reflects the advantages of PWPf modulation over bangbang control.

To reduce the thruster firing when bangbang control is used, the case of bangbang controller employing a deadzone is also tested. The deadzone is set from -0.45 to $+0.45$, which corresponds to the data for the PWPf modulator. The active vibration suppression sub-system is implemented in this case. Severe rigid body and flexible appendage interaction is observed. The vibrations of rigid body and the flexible appendage are reflected in Fig. 16. Even with a deadzone, the bangbang control still uses more fuel and more number of firings than PWPf modulated thruster control, as shown in Fig. 17. This further demonstrates the superiority of attitude control using PWPf modulation over bangbang control with or without a deadzone.

To demonstrate the effect of the active vibration suppression using smart structures, a 30° slew of the FSS using PWPf modulator with active vibration suppression sub-system turned off is conducted. The control parameters for the attitude control sub-system remain the same for a fair comparison. Since the active vibration suppression sub-system is turned off, no active damping will be provided to the flexible appendage from the PZT patches. As compared with Fig. 11 when active vibration suppression sub-system is on, the vibrations observed in Fig. 18 are more severe. This observation is quantified from the PSD plots in Fig. 13. Since the PPF control only targets at the 1st and 2nd modes, it is reasonable to see that the 3rd mode vibrates at the same energy level in either case. With the PPF control turned on, the 2nd mode energy level is brought down by 15 dB, while the 1st mode's is decreased by 4 dB. This shows the effectiveness of the smart structure along with PPF control for active vibration suppression.

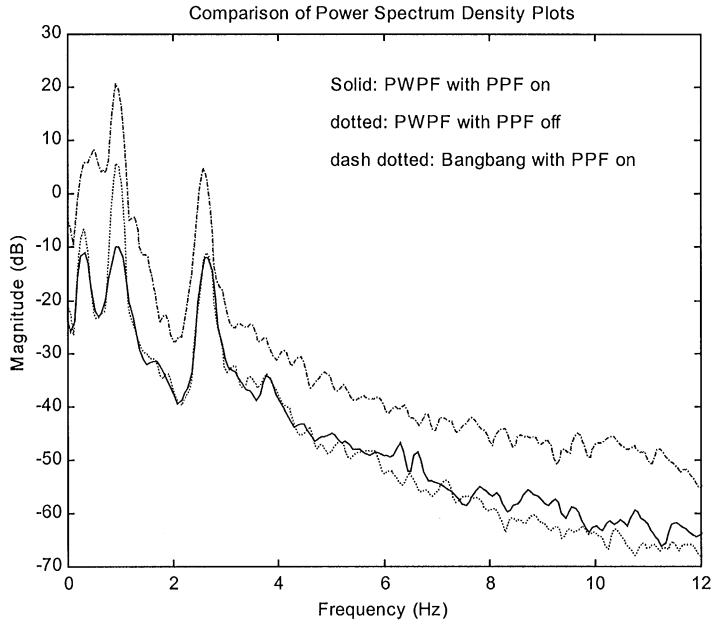


Fig. 13. Comparison of power spectrum density plots.

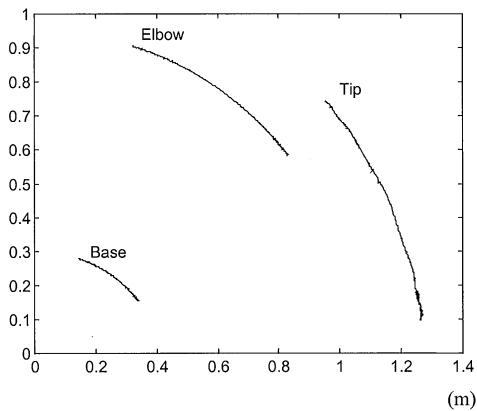


Fig. 14. Trace of the flexible appendage movement during a 30° slew with PWWF modulation and active vibration suppression.

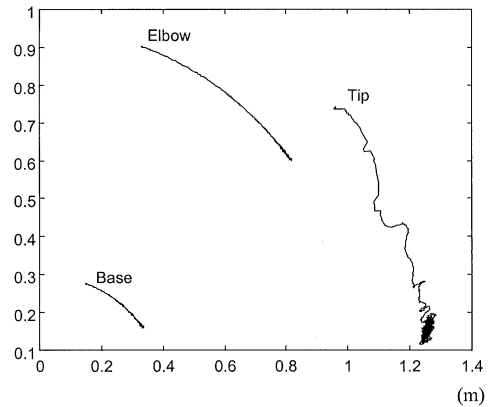


Fig. 15. Trace of the flexible appendage movement during a 30° slew with bangbang control (no deadzone) and active vibration suppression.

6.2. Station keeping

In this experiment, FSS station keeping tasks are performed. To demonstrate the advantages of the PWWF modulator over the bangbang control, attitude controls using both methods are conducted. In both cases, the same active vibration suppression sub-system is used to counter react to the thruster-firing-induced vibrations on flexible appendage. The PD controller employs the same gains during both tests for a fair complexion.

First, the FSS under attitude control via PWWF modulation is tested. At $t = 10$ s, a disturbance is introduced to the FSS so that the rigid body devi-

ated about 7° from its desired position, 29.5° , as shown in Fig. 19. In about 15 s, the orientation of FSS rigid body converges to around 29.5° with little overshoot. At the steady state, 0.5° error in orientation is observed. Little vibrations on the flexible appendage are observed, as indicated by the voltage outputs of PZT sensors located at both the base and remote beams. These voltage outputs are also shown in Fig. 19.

On the other side, when the bangbang control is used in the attitude control sub-systems, the FSS system experiences instability after a disturbance is introduced to it, as shown in Fig. 20. Violent vibrations on the flexible appendage are also

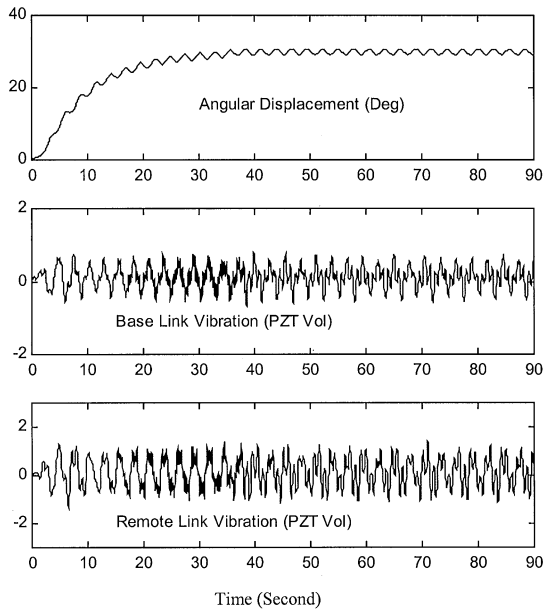


Fig. 16. Slew with bangbang control (with deadzone) and active vibration suppression.

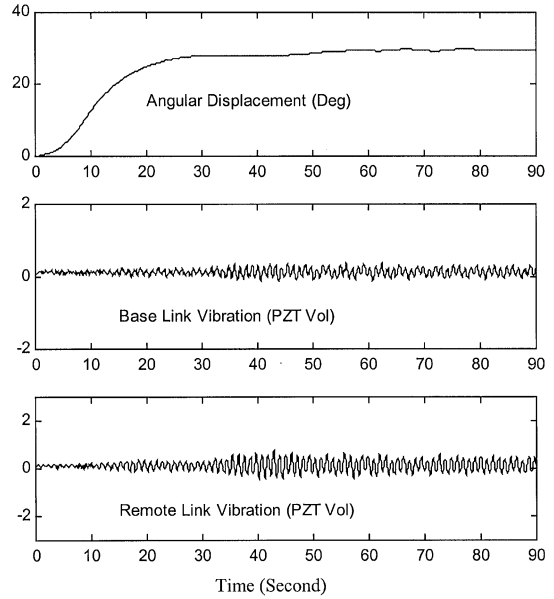


Fig. 18. Slew with PWPF modulation but without active vibration suppression.

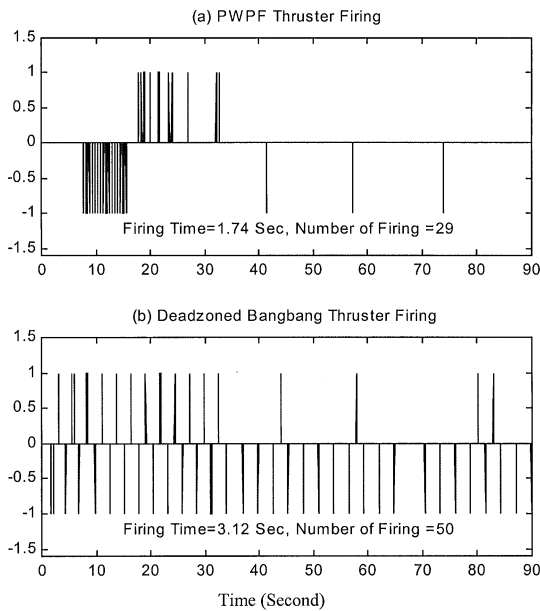


Fig. 17. Thruster firing comparison between (a) PWPF modulation and (b) deadzoned bangbang control.

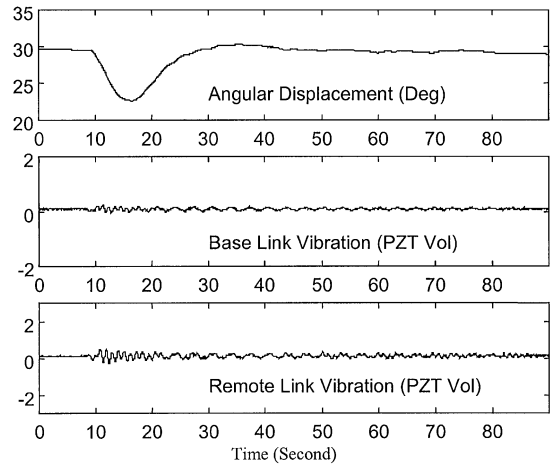


Fig. 19. Station keeping using PWPF modulator.

7. CONCLUSIONS

observed, as confirmed by the PZT sensors voltage outputs shown in Fig. 20. Comparison of the two experiments clearly demonstrates the superiority of PWPF modulation over bangbang control during station keeping tasks.

This paper proposes a new approach to vibration reduction of flexible spacecraft during attitude maneuver. In this approach, the PWPF modulation is used to control thruster firing in the attitude control system to reduce vibrations introduced to the flexible structure, meanwhile, on the other hand, smart structures are employed to actively suppress vibrations induced by thruster firing. Experimental results of attitude control of the US Naval Postgraduate School’s flexible spacecraft simulator (FSS) using this approach demonstrate that the use of the PWPF modulator reduces vibration, improves pointing accuracy, and reduces fuel consumption

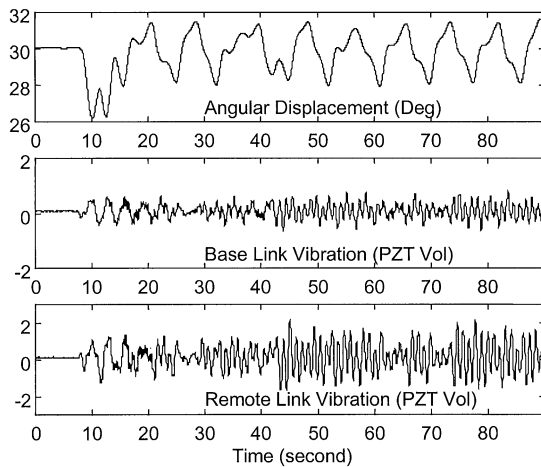


Fig. 20. Station keeping using bangbang Control.

as compared to bangbang control with or without a deadzone. Experiments also demonstrate smart structures with positive position feedback (PPF) provides actively damping to the flexible structure and helps to increase point accuracy and reduce fuel consumption. Overall, the method of vibration reduction of flexible spacecraft during attitude control using PWPF modulator and smart structures is demonstrated effectively.

Acknowledgements—The authors would like to thank Dr. T. Huang, Dr. G. Ramirez, Major S. Edwards, and LT. B. Kelly for their assistance in conducting a portion of the FSS experiment.

REFERENCES

1. Millar, A. and Vigneron, F. R., Attitude stability of flexible spacecraft which use dual time constant feedback lag network pseudorate control. *AIAA/CASI 6th Communications Satellite Systems Conference, Montreal, Canada*, April, 1976.
2. Clark, R. N. and Franklin, G. F., Limit cycle oscillations in pulse modulated systems. *Journal of Spacecraft and Rockets*, 1969, **6**, 799–804.
3. Hablani, H. B., Multiaxis tracking and attitude control of flexible spacecraft with reaction jets. *AIAA Journal of Guidance, Control, and Dynamics*, 1994, **17**, 831–839.
4. Bittner, H., Fischer, H. D. and Surauer, M., *Design of Reaction Jet Attitude Control Systems for Flexible Spacecraft*. IFAC Automatic Control in Space, Noordwijkerhout, The Netherlands, 1982.
5. Wie, B. and Plescia, C. T., Attitude stabilization of flexible spacecraft during station keeping maneuvers. *Journal of Guidance, Control, and Dynamics*, 1989, **7**, 430–436.
6. Anthony, T., Wei, B. and Carroll, Pulse-modulated control synthesis for a flexible spacecraft. *AIAA Journal of Guidance, Control, and Dynamics*, 1990, **13**, 1014–1015.
7. Song, G., Buck, N. and Agrawal, B., Spacecraft vibration reduction using pulse-width pulse-frequency modulated input shaper. *AIAA Journal of Guidance, Control, and Dynamics*, 1999, **22**, 433–440.
8. Goh, C. J. and Caughey, T. K., On the stability problem caused by finite actuator dynamics in the collocated control of large space structure. *International Journal of Control*, 1985, **41**, 787–802.
9. Fanson, J. L. and Caughey, T. K., Positive position feedback control for large space structure. *AIAA Journal*, 1990, **28**, 717–724.
10. Agrawal, B. N. and Bang, H., Adaptive structure for large precision antennas. *45th Congress of the International Astronautical Federation*, Jerusalem, Israel, October, 1994.
11. Meyer, J., Harrington, B., Agrawal, B. and Song, G., Vibration suppression of a spacecraft flexible appendage using smart material. *Institute of Physics Journal of Smart Material and Structures*, 1998, 95–104.
12. Song, G., Schmidt, S. and Agrawal, B. N., Experimental study of vibration suppression of flexible structure using modular control patch. *Proceedings of IEEE Aerospace Conference*, Snowmass, CO, 1998.
13. Buck, N. V., Minimum vibration maneuvers using input shaping and pulse-width pulse-frequency modulated thruster control. Master Thesis, US Naval Postgraduate School, December, 1996.